AJNR

CT Perfusion Quantification of Small-Vessel Ischemic Severity

T.J. Huynh, B. Murphy, J.A. Pettersen, H. Tu, D.J. Sahlas, L. Zhang, S.P. Symons, S. Black, T.-Y. Lee and R.I. Aviv

T.J. Huynh
B. Murphy
J.A. Pettersen
H. Tu
D.J. Sahlas
L. Zhang
S.P. Symons
S. Black
T.-Y. Lee
R.I. Aviv

CT Perfusion Quantification of Small-Vessel Ischemic Severity

BACKGROUND AND PURPOSE: Cerebral blood flow (CBF) abnormalities are previously demonstrated in white matter disease. A gradation of change may exist between patients with mild and more severe white matter disease. An association between blood brain barrier dysfunction, increasing age and white matter disease is also suggested. The purpose of this study was to quantify and correlate white matter disease severity and CT perfusion (CTP)-derived CBF and to determine whether permeability surface abnormality increases with white matter disease severity.

MATERIALS AND METHODS: One hundred twenty patients with strokelike symptoms underwent CTP and MR imaging. Of these, 35 patients (15 women, 20 men; age, 66 ± 15.7 years) with rapidly resolving symptoms and normal imaging characteristics consistent with transient ischemic attack were retrospectively reviewed and constituted the study cohort. Two blinded neurologists rated white matter severity, assigning age-related white matter change (ARWMC) scores. Patients were dichotomized a priori into mild and moderate-to-severe. CBF, cerebral blood volume (CBV), mean transit time (MTT), and permeability surface product maps were calculated for periventricular and subcortical white matter regions and average white and gray matter. Associations with white matter severity were tested by uni- and multivariate logistic regression analyses. Receiver operating characteristic analysis was performed.

RESULTS: White matter disease was mild in 26 patients and moderate-to-severe in 9. Age was associated with increased likelihood of having moderate-to-severe white matter disease ($P = .02$). ARWMC correlated with subcortical ($r = -0.50$, $P < .001$) and average CBF ($r = -0.55$, $P < .001$). White matter severity was associated with subcortical ($P = .03$) and average ($P = .03$) white matter CBF, with a trend toward periventricular white matter CBF ($P = .05$). Uni- and multivariate analysis controlling for the confounding effect of age demonstrated significant association between white matter severity and subcortical ($P = .032$) white matter CBF. Area under the curve was 0.82. No permeability surface abnormality was found.

CONCLUSIONS: CTP-derived subcortical white matter CBF is independently associated with white matter disease severity.

White matter changes are frequent in patients with vascular risk factors, cerebrovascular disease, and cognitive impairment.[1] The pathogenesis is poorly understood. Various histopathologic correlates have been described, including loss of ependyma with gliosis, glial swelling, demyelination, dilated perivascular spaces, lacunar infarcts, spongiosis, arteriolar hyalinosis, amyloid angiopathy, and cyst formation.[2-4] A vascular etiology is strongly suggested, given the frequent association with increasing age, hypertension, stroke, and markers of cellular ischemia, including hypoxia inducible factor, neuroglobulin, and matrix metalloproteinase protein MMP7.[5-7] Other associations include arteriosclerosis,[8] impaired cerebral autoregulation, hypoperfusion, CSF flow disturbances, and blood-brain barrier (BBB) disruption.[7,9]

Several validated white matter rating scales allow visual quantification of disease burden on CT or MR imaging. The age-related white matter change (ARWMC) scale can be ap-

plied to both CT and MR imaging changes and has been recommended in an attempt to standardize nomenclature in vascular cognitive impairment imaging.[10] White matter lesion visualization is, however, reduced on CT compared with MR imaging. Additionally, visual rating score performances are imperfect and are limited by a ceiling effect. The wide variation in lesion extent with high visual scores results in a lower correlation with clinical symptoms. Whether techniques that provide estimation of white matter hemodynamic parameters independent of CT or MR imaging lesion visualization would better assess severity is unknown but potentially may circumvent these problems.

Cerebral blood flow (CBF) abnormalities were previously demonstrated in white matter disease by xenon CT (Xe-CT),[11] positron-emission tomography (PET),[12] and MR imaging.[13,14] Correlation of XeCT and single-photon emission tomography (SPECT) hypoperfusion with leukoaraiosis severity was previously described.[11,15] Recent data suggest that hemodynamic alterations precede white matter change.[16] An association between BBB dysfunction, increasing age, dementia, and white matter disease is suggested, with parenchymal gadolinium-diethylene-triamine pentaacetic acid leakage shown in elderly patients with diabetes.[17] Furthermore, microvascular changes, BBB dysfunction, and microglial and astroglial cell activation are reported in primates with cognitive decline.[18] Progress in cross-sectional CT imaging technology allows quantification of absolute cerebral hemodynamic parameters with greater resolution than MR imaging or SPECT-
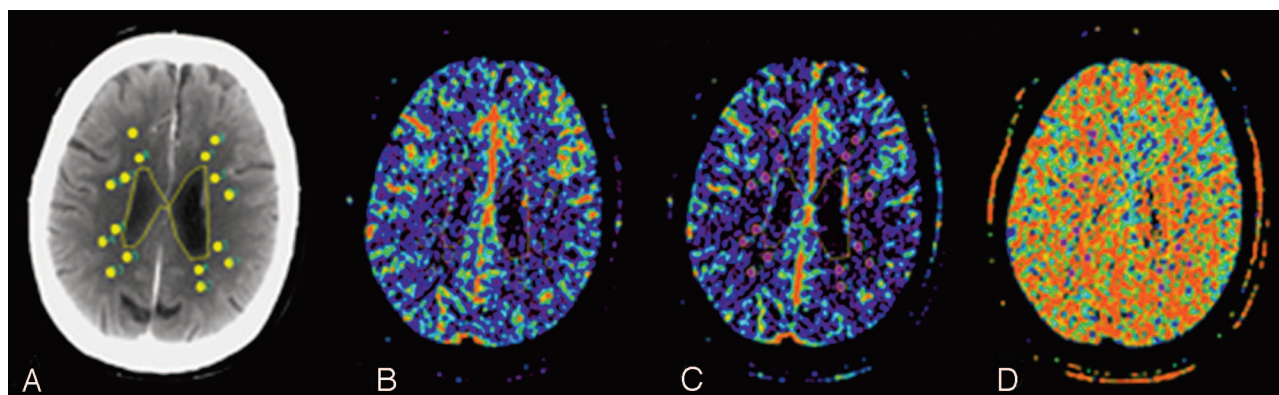
Fig 1. Region-of-interest technique for perfusion determination. Two ROIs are drawn on the average map (*A*) adjacent to each ventricle for a total of 8 PV ROI's. Two further ROIs are placed within the adjacent subcortical white matter defined by an imaginary line between the ventricle and overlying cortex for a total of 8 SC ROIs. The ROIs are subsequently projected onto the inherently coregistered maps for PV and SC CBF (*B*), CBV (*C*) and MTT (*D*) calculation.

based techniques. CT perfusion (CTP) is cheaper, faster, and more widely available than MR imaging, SPECT, or Xe-CT techniques. CTP is widely used in the evaluation of patients with stroke, but no previous study has examined the relationship between CTP-derived hemodynamic variables and white matter disease severity. The purpose of this study was to test the ability of CTP-derived hemodynamic parameters, including CBF, cerebral blood volume (CBV), mean transit time (MTT), and BBB permeability surface product to quantify white matter disease severity. Our hypothesis was that CTP-derived hemodynamic parameters and, in particular, CBF correlate with and may be used to quantify white matter disease severity. Furthermore, we hypothesized that permeability surface is expected to increase with greater white matter disease severity.

Materials and Methods

Patients

All patients presenting to our tertiary stroke center within 3 hours of acute onset between January 2006 to July 2007 undergoing our routine CT stroke protocol (including CT angiography [CTA] and CTP) were considered for inclusion in this study. Patients with any carotid stenosis on CTA or ischemia/infarct on perfusion imaging or diffusion-weighted imaging were excluded. Of a total of 120 prospectively acquired patients, 40 demonstrating mild initial stroke symptoms with rapid clinical improvement (ie, transient ischemic attack) before the baseline CT study were included for retrospective study. Five patients were excluded after enrollment due to concomitant head trauma ($n = 1$) and excessive movement ($n = 4$). The study was approved by the institutional review board, and all participants provided informed consent at the time of their admission.

Imaging

The CT stroke protocol was performed on a 4- or 64-section CT scanner (LightSpeed VCT; GE Healthcare, Milwaukee, Wis). Components included pre- and postcontrast head CT from the skull base to the vertex with the following imaging parameters: 120 kilovolt (peak), 340 mA, 4 × 5 mm or 8 × 5 mm collimation, 1 s/rotation; table speed of 15 mm/rotation. CTP comprised 2 phases with the following parameters: 80 kVp, 190 mA, 3- to 5-second delay, injection of 0.5-mL/kg (30–50 mL) Iohexol (300 mg I/mL, Omnipaque; Nycomed, Princeton, NJ) at 4 mL/s. The initial phase consisted of a 45-second

cine scanning at 1 rotation/s. After June 2006, a second phase was added with 1 rotation/s every 15 seconds for an additional 75 seconds.

Sixteen patients underwent the extended protocol from which permeability surface product (permeability) was derived.[19] All CTP studies covered a 20- to 40-mm slab with 4 to eight 5-mm sections, centered between the anterior commissure and the centrum semiovale. Arterial and venous time-enhancement curves were obtained from the anterior cerebral artery and the superior sagittal sinus, respectively. CTP 3 software (GE Healthcare) was used to calculate the CBF, CBV, MTT, and permeability surface parametric maps by deconvolution of 2 × 2 pixels. Deconvolution-derived CBF and CBV CT imaging has been shown to be quantitative and accurate when compared with PET or Xe-CT imaging.[20,21] Arterial input and venous output functions were obtained from the anterior cerebral artery and from the superior sagittal sinus, respectively. Partial volume averaging of the arterial input curve was corrected by using the venous time-enhancement curve. Perfusion-weighted (PW) maps were calculated by averaging cine images over the duration of the first contrast passage through the brain. Permeability maps were obtained by using CTP 4 software (GE Healthcare) requiring data from a 2-phase acquisition. Delayed-phase imaging allows the permeability surface map to be calculated by modeling the first pass of the contrast and then assessing the degree of contrast extravasation. Persistence of contrast within a voxel after the passage of the bolus is indicative of BBB leakage and reflects in an elevated permeability surface product. The calculations are performed at the same 2 × 2 pixel block as the CBF and CBV calculations

Image Analysis

Functional maps (PW, CBF, CBV, MTT, and permeability surface) were imported into custom software (IDL v5.G; RSI, Boulder, Colo) for analysis. A region-of-interest technique and a previously described automatic threshold–based technique were used to collect data from the functional maps (Fig 1*A*, -*B*).[22,23] Analysis was performed at the level of the superior portion of the lateral ventricles for all patients according to the template shown in Fig 1. This region is routinely covered irrespective of CTP coverage obtained (2–4 cm). Equal sized regions of interest (36 pixels) were placed in prespecified periventricular and subcortical locations on the PW map (Fig 1) in every patient. Periventricular-location selection was based on those regions where white matter changes are most frequently seen. Eight periventricular regions of interest were placed around the anterior

Table 1: Age-related white matter change scale*

Location	Characteristics†
White matter	
0	No lesions (including caps/bands)
1	Focal lesions
2	Beginning confluence of lesions
3	Diffuse involvement of the entire region, irrespective of U fiber involvement
Basal ganglia	
0	No lesions
1	1 focal lesion (≥5 mm)
2	>1 focal lesion
3	Confluent lesions

* Brain regions assessed included frontal, parieto-occipital, temporal, infratentorial/cerebellum, and basal ganglia (striatum, globus pallidus, thalamus, internal/external capsule, and insula).
† White matter changes on MR imaging are defined as bright lesions ≥5 mm on T2, proton-density, or fluid-attenuated inversion recovery images. Lesions on CT were defined as hypodense areas of ≥5 mm; left and right hemispheres were rated separately.

Table 2: Spearman correlation (*r*) between CTP variables and age-related white matter change scale MRI score

CTP Variables		MRI Score	*r* (*P* value)
Blood Flow (*n* = 35)	Periventricular WM	−0.55	(<.01)
	Subcortical WM	−0.50	(<.01)
	Average WM	−0.55	(<.01)
	Average GM	−0.43	(<.01)
Blood volume (*n* = 35)	Periventricular WM	−0.23	(.18)
	Subcortical WM	−0.050	(.78)
	Average WM	−0.15	(.39)
	Average GM	0.024	(0.89)
MTT (*n* = 35)	Periventricular WM	0.45	(<.01)
	Subcortical WM	0.43	(<.01)
	Average WM	0.31	(.07)
	Average GM	0.37	(.03)
PS product (*n* = 16)	Periventricular WM	−0.20	(.46)
	Subcortical WM	−0.22	(.41)
	Average WM	−0.01	(.9)

Note:—MRI indicates MR imaging; WM, white matter; GM, gray matter; PS, permeability surface product; MTT, mean transit time; CTP, CT perfusion.

and posterior horns of the lateral ventricles: 4 surrounding the frontal horns and 4 surrounding the posterior horns. Eight subcortical-location regions of interest were uniformly distributed through the subcortical white matter, lateral to an imaginary line between the ventricle and overlying cortex.[13] Region-of-interest placements were independently verified by a blinded reader (who was an experienced neuroradiologist) to ensure that no CSF or gray matter structures were included. To minimize partial volume effects, we placed regions of interest at least 2 mm from tissue boundaries. No reproducibility measures for region-of-interest placement were assessed in this study.

The average white matter value was obtained by calculating the mean of periventricular and subcortical region-of-interest values. CBF and CBV thresholds of >100 mL$^{-1} \cdot$ min$^{-1} \cdot$ 100 g^{-1} or >8 mL $\cdot$ 100 g^{-1}, respectively, were applied to perfusion maps to minimize the vascular pixel contribution. It has been shown that CTP values correlate well with Xe-CT and PET when large vessels are excluded.[20,21] A semiautomated threshold technique based on Hounsfield units was used to create a whole gray matter mask on the PW images.[22,23] This mask was then applied to the functional maps to derive mean gray matter CBF, CBV, MTT, and permeability surface product values.

ARWMC Rating
The ARWMC score was used to grade white matter disease severity according to a technique that was previously published.[24] Scores of 0–3 are applied to each frontal, parietooccipital, and temporal white matter region and both basal ganglia for a total score of 30 (Table 1). Scores were calculated independently on emergent MR imaging typically performed 1–2 days after CT by 2 neurologists blinded to other data and then averaged.

Statistical Analysis
Results were expressed as the mean ± SD and median (interquartile) for quantitative variables and as proportions for categoric data. Histograms were superimposed on fitted normal curves to test normalization of data distribution. Those variables that were not normalized were subject to logarithmic transformation. A log-transformation was applied to several variables to normalize their distributions. Spearman correlations (*r*) were calculated between ARWMC MR imaging scores and multiple functional parameters, such as CBF, CBV, MTT, and permeability surface product, for the periventricular and subcortical regions of interest and the gray matter. Patients were di-

chotomized a priori into mild (WM^m) and moderate-to-severe white matter disease (WM^{ms}) groups by using an ARWMC score of ≤7 as a cutoff. On the basis of the sample size, the study was powered to detect a CBF difference of 4 mL/100 g/min with 90% power and α level <0.05. The Wilcoxon rank sum test or the Fisher exact test was used to compare the difference between WM^m and WM^{ms} on demographic data and CTP variables.

Intra- and intergroup comparisons of periventricular and subcortical CBF and CBV were made. Association between white matter severity and demographic or CTP variables was tested by uni- and multivariate logistic regression analysis with adjustment for age as a confounding factor. A stepwise logistic regression analysis (inclusion criteria of $P < .05$ and exclusion criteria of $P > .05$) was performed to determine the variables predictive of white matter severity. A Bonferroni correction was not performed because only a single outcome measure of white matter severity was used and because of the preliminary and exploratory nature of this study. Odds ratios (OR) with 95% confidence intervals were calculated. The efficacy of the model was appraised by receiver operator characteristic (ROC) analysis, including area under the curve, sensitivity, and specificity. The best cutoff threshold was chosen by the highest sensitivity and specificity. The effects of age and subcortical CBF on the probability of developing positive white matter disease were computed by using a risk function of probability. The risk function (*Rf*) indicates the probability of having WM^{ms} with the calculated CBF threshold. A *Rf* was derived by predicted factors as follows: $Rf = 0.098 \times$ age $+3.34 \times$ subcortical CBF, with a cutoff point of 10.1 ± 4.31. Subcortical CBF was coded 0 for >11.9 mL/100 g/min and 1 for $≤11.9$ mL/100 g/min. The greater the value of *Rf*, the higher is the risk of developing positive white matter. A $P < .05$ was considered statistically significant, and all calculations were performed by using SAS (Version 9.1 for Windows; SAS Institute, Cary, NC) statistical software.

Results
Thirty-five patients (mean age, 66 ± 15.7 years) were analyzed (20 men and 15 women). The median ARWMC MR imaging score was 5 (interquartile range [IQR], 2–8). Median National Institutes of Health Stroke Scale score at presentation was 5 (IQR, 2–8) and at discharge, 0.5 (IQR, 0–2). The Spearman correlation between MR imaging score CBF, CBV, MTT, and permeability surface in white matter regions of interest and

Table 3: Demographics in total patients and in patients with WM^m or WM^ms

	Total (*n* = 35)	WM^ms (*n* = 9)	WM^m (*n* = 26)	*P* Value*
Age (yr; mean ± SD)	66.3 ± 15.7	77.1 ± 6.0	62.6 ± 16.3	.02
Sex (No., % male)	15 (42.9%)	5 (55.6%)	10 (38.5%)	.45
Smoking (No., %)	3 (8.6%)	0 (0%)	3 (11.5%)	.56
Cardiovascular disease (No., %)	7 (20.0%)	2 (22.2%)	5 (19.2%)	.85
Hypertension (No., %)	3 (8.6%)	2 (22.2%)	1 (3.9%)	.16
Hyperlipidemia (No., %)	11 (31.4%)	2 (22.2%)	9 (34.6%)	.69
Diabetes (No., %)	2 (5.7%)	1 (11.1%)	1 (3.9%)	.45
Presentation NIHSS median (IQR)	5 (2–8)	4 (1–6)	5 (2–8)	.43
Discharge NIHSS (median)	0.5 (−2)	0.5 (0–2.5)	0.5 (0–1)	.81
ARWMC MRI score median (IQR)		12 (8–15)	3 (2–5)	

Note:—NIHSS indicates National Institutes of Health Stroke Scale; MRI, MR imaging; WM^m, mild white matter disease; WM^ms, moderate-to-severe white matter disease; ARWMC, age-related white matter change.
* Obtained by the Wilcoxon rank sum test or the Fisher exact test. *P* < .05 was considered as significant.

Table 4: CTP variables in patients with WM^m and WM^ms without adjusting for age as a confounding factor

CTP Variables	WM^ms (mean, SD)	WM^m (mean, SD)	*P* Value*
Blood flow (mL/100 g/min)	*n* = 9	*n* = 26	
Periventricular WM	11.4 (3.3)	15.7 (3.4)	<.01
Subcortical WM	10.9 (2.8)	15.3 (3.7)	<.01
Average WM	11.2 (2.9)	15.5 (3.3)	<.01
Average GM	27.7 (6.4)	33.9 (6.9)	.02
Blood volume (mL/100 g)	*n* = 9	*n* = 26	
Periventricular WM	0.7 (0.2)	0.9 (0.3)	.01
Subcortical WM	0.8 (0.2)	0.9 (0.5)	.28
Average WM	0.8 (0.2)	0.9 (0.4)	.03
Average GM	1.5 (0.4)	1.7 (0.3)	.40
MTT (seconds)	*n* = 9	*n* = 26	
Periventricular WM	0.07 (0.01)	0.06 (0.02)	.24
Subcortical WM	0.07 (0.02)	0.06 (0.02)	.06
Average WM	0.06 (0.01)	0.06 (0.02)	.22
Average GM	0.06 (0.01)	0.05 (0.01)	.34
Permeability (mL/min/100 g)	*n* = 6	*n* = 10	
Periventricular WM	0.01 (0.01)	0.01 (0.008)	.42
Subcortical WM	0.02 (0.017)	0.01 (0.01)	.99
Average WM	0.01 (0.01)	0.01 (0.01)	.86

Note:—WM indicates white matter; GM, gray matter; WM^ms, moderate-to-severe white matter disease; WM^m, mild white matter disease.
* Obtained by the Wilcoxon rank sum test. *P* < .05 was considered as significant.

gray matter is presented in Table 2. There was significant inverse correlation between the ARWMC MR imaging score and periventricular CBF ($r = -0.55$, $P < .01$), subcortical CBF ($r = -0.50$, $P < .01$), average white matter CBF ($r = -0.55$, $P < .01$), and GM CBF ($r = -0.43$, $P < .01$). A positive correlation was shown between the ARWMC MR imaging score and periventricular MTT ($r = 0.45$, $P < .01$), subcortical MTT ($r = 0.43$, $P < .01$), and gray matter MTT ($r = 0.37$, $P = .03$). No correlation between the ARWMC score, permeability surface product, or CBV was found.

There were 26 patients with WM^m and 9 patients with WM^ms. Table 3 shows median ARWMC MR imaging scores in each group. No significant differences in intergroup baseline demographic characteristics, including cardiovascular risk factors, were present, apart from age. Older patients were more likely to have WM^ms disease than younger patients ($P = .02$). Hemodynamic differences are given in Table 4. All CBF variables, periventricular white matter, and average white matter CBV were significantly lower in the WM^ms versus WM^m group. Other CTP variables did not differentiate between the 2 groups. Hemodynamic differences between

periventricular and subcortical locations were not demonstrated.

Univariate logistic regression analysis, adjusting for age, revealed that white matter severity was significantly associated with CBF in the subcortical white matter ($P = .03$) and average white matter ($P = .03$) and a trend toward periventricular white matter ($P = .05$) (Table 5). Periventricular blood volume ($P = .03$) and average white matter CBV ($P = .03$) were also significant predictors of white matter severity, but age remained a significant confounder.

Stepwise multivariate logistic regression analysis demonstrated a significant negative association between subcortical CBF and white matter disease probability ($P = .03$, OR = 0.635). A subcortical white matter CBF threshold of ≤11.9 mL/100 g/min demonstrated an area under the ROC curve, sensitivity, specificity, and positive likelihood ratio of 0.82, 89% (52%–98%), 77% (56%–91%), and 3.9, respectively. To illustrate the effects of age and subcortical CBF on the probability of developing positive white matter, we considered 2 patients 65 and 70 years of age. The probability of WM^ms disease increased from 40% to 52% when age increased from 65 to 70 years with a subcortical CBF ≤11.9 mL/100 g/min. The same patients with subcortical CBF of >11.9 had a risk of 2.4% and 3.8%, respectively. This finding confirms that subcortical CBF has much more effect on the probability of positive white matter than age.

Discussion

CBF was lower in periventricular and subcortical white matter regions in patients with WM^ms, compared with those patients with less disease burden. Subcortical white matter, but not periventricular white matter CBF, was independently associated with white matter disease severity represented by the ARWMC score, with good sensitivity and specificity. No permeability changes were demonstrated between the 2 white matter disease groups.

Sensitivity for white matter detection on noncontrast CT is lower than that on MR imaging. Potentially, subcortical CBF measures may overcome the limitation of noncontrast CT white matter burden estimation. CTP has some advantages over MR imaging perfusion: It can be performed by all clinical multidetector CT scanners and provides quantitative data on cerebral hemodynamic variables including CBF, CBV, MTT, and permeability surface. Concerns over radiation doses are frequently cited, especially if the technique is used for longitu-

Table 5: CTP variables predictive of WM disease after adjusting for age confounder, as obtained by the univariate logistic regression analysis ($n = 35$)

	CTP Variables		Age Confounder	
	P Value	OR (95% CI)	P Value	OR (95% CI)
CBF				
Periventricular WM	.05†	0.727 (0.529–0.999)	.195†	1.062 (0.970–1.163)
Subcortical WM	.03†	0.635 (0.419–0.963)	.069†	1.094 (0.993–1.205)
Average WM	.03†	0.644 (0.457–0.964)	.145†	1.069 (0.977–1.171)
Average GM	.20	0.916 (0.802–1.047)	.099	1.083 (0.985–1.190)
CBV				
Periventricular WM	.03‡	0.992 (0.986–0.999)	.043‡	1.112 (1.003–1.233)
Subcortical WM	.06	0.995 (0.989–1.000)	.023	1.132 (1.017–1.259)
Average WM	.03‡	0.993 (0.986–0.999)	.027‡	1.128 (1.014–1.256)
Average GM	.20	0.998 (0.995–1.001)	.035	1.101 (1.007–1.205)
MTT				
Periventricular WM	.86‡	0.938 (0.470–1.870)	.048‡	1.103 (1.001–1.216)
Subcortical WM	.24	1.335 (0.826–2.158)	.043	1.095 (1.003–1.196)
Average WM	.99‡	0.995 (0.442–2.242)	.040‡	1.120 (1.005–1.248)
Average GM	.97	1.011 (0.553–1.848)	.035	1.100 (1.005–1.203)

Note:—CI indicates confidence interval; WM, white matter; GM, gray matter; CBV, cerebral blood volume; MTT, mean transit time; CBF, cerebral blood flow; CTP, CT perfusion.
† CTP variable is significant ($P < .05$) when the age confounder is not related to the disease.
‡ CTP variable is significant ($P < .05$) when the age confounder is related to the disease.

dinal follow-up. A recent study confirmed that the radiation dose delivered by a CTP study is less than that of a conventional noncontrast CT because of a small field of coverage and the use of gantry tilting to avoid orbital radiation.[25] The radiation dose is associated with <0.01% lifetime attributable risk of cancer-induced death.[26] Furthermore, a number of patients may not be able to undergo MR imaging due to claustrophobia, intolerance of longer scanning times, and other MR imaging contraindications. CT is also widely available, making it an attractive method for assessing white matter disease severity. A drawback of CTP is the limited coverage of 2–4 cm; however, this may be improved with a table-toggle technique.

We observed that subcortical CBF values for patients with WM[m] are lower than the published values of normal white matter in patients without white matter disease.[13] Subcortical CBF in WM[m] is consistent with values for normal-appearing white matter in patients with existing white matter disease.[13] Our results indicate that the degree of hypoperfusion within the subcortical location increases with ARWMC score severity and is abnormal even in those patients with mild disease. These findings support the hypothesis that hypoperfusion may precede the onset of white matter change. Emergence of signal-intensity abnormality on MR imaging is presumably a more advanced manifestation of underlying white matter hypoperfusion. Although perfusion techniques in white matter disease are currently experimental, our results and those of others suggest that CBF may be a useful surrogate marker of white matter disease severity.[12,27,28] This finding may have potential important clinical implications for monitoring hemodynamic response in the context of pharmacologic intervention in white matter disease.

Periventricular CBV reduction was associated with increased white matter disease severity but correlated poorly with ARWMC score. Two previous studies examining a small number of patients (17 and 23 patients) did not find significant differences in CBV between patients with and without white matter disease.[12,28] Lower periventricular CBV in patients with WM[ms] could be explained by differences in the autoregulatory capacity between patients with WM[m] and

WM[ms]. Under normal circumstances, CBF reduction may be accompanied by an increased oxygen extraction fraction and vasodilation (CBV elevation).[29] These changes are demonstrated in asymptomatic patients with white matter disease.[12] Autoregulatory dysfunction occurs due to progressive vascular arteriosclerosis, resulting in perforator territory vessel lumen reduction and concomitant CBF reduction.[8,14,28] Vessel wall thickening, endothelial cell activation, and dysfunction contribute to autoregulatory dysfunction[30,31] and CBV reduction. The effect of autoregulatory dysfunction is more likely to be detected within the periventricular region because it represents a deep borderzone between centrifugal subependymal and centripetal penetrating medullary vessels. The lesser degree of autoregulatory dysfunction within the subcortical white matter may be explained by the lower susceptibility of this region to hypoperfusion compared with periventricular regions.

Cortical (gray matter) CBF reduction was seen in both groups. The effect was independent of white matter disease severity and was confounded by age. This finding supports a previous study suggesting that white matter hypoperfusion is a primary etiology in white matter disease rather than secondary to cortical hypometabolism.[13] CT permeability imaging is a novel method of measuring permeability and has been shown to be successful in tumor imaging,[32] with a growing experience in stroke imaging.[33] Despite a suggested putative link between permeability changes and the development of white matter changes,[16,31] we were unable to demonstrate any significant differences in BBB permeability in periventricular or subcortical white matter for patients with white matter disease. However, the number of patients studied here was small. Whether the technique is sensitive enough to detect the magnitude of changes thought to be present in chronic white matter ischemia[16] remains to be determined.

A potential limitation of our study was the method of patient cohort selection. However, the absence of any acute or follow-up imaging abnormality and the concordance of hemodynamic results with other white matter studies argue against the CBF reductions being caused by clinical presenta-

tion. A further limitation is the small number of patients within the WM^{ms} group. We chose to measure periventricular and subcortical perfusion change by using a region-of-interest–based technique. This technique may be criticized for not favoring regions where white matter changes are most severe. The region-of-interest template applied to all patients was the best way, in our view, to standardize the number and location of regions of interest across all patients. Region-of-interest placement did take into account regions where white matter changes are expected to be most severe and avoided haphazard region-of-interest placement and numbers. We believe that this methodology makes our findings more robust because we did not attempt to target specifically the worst areas affected.

The methodology is limited by no attempt being made to assess interobserver variability. We are confident that little variation in region-of-interest placement occurred because all regions of interest were checked by the same experienced neuroradiologist. Ideally, we preferred to have assessed the correlation of CBF with neurocognitive data rather than an MR imaging score; however, these data were not available. A recent study has shown utility for CTP-derived CBF and CBV in distinguishing Alzheimer disease from vascular dementia.[34] It remains to be determined whether CTP hemodynamic variables correlate with cognition in addition to white matter scores.

Conclusions
There is a fair correlation between subcortical CBF assessment and white matter disease severity. Subcortical white matter CBF is independently associated with white matter disease severity. Whether CTP has a role in the longitudinal assessment of white matter patients or as a surrogate marker of response to drug interventions remains to be determined. We hope to assess these parameters in prospectively acquired patient cohorts and correlate findings with neurocognitive outcome in addition to imaging-based white matter scores.

References
1. Breteler MM, van Swieten JC, Bots ML, et al. **Cerebral white matter lesions, vascular risk factors, and cognitive function in a population-based study: the Rotterdam Study.** *Neurology* 1994;44:1246–52
2. Inzitari D, Mascalchi M, Giordano GP, et al. **Histopathological correlates of leuko-araiosis in patients with ischemic stroke.** *Eur Neurol* 1989;29(suppl 2):23–26
3. Scarpelli M, Salvolini U, Diamanti L, et al. **MRI and pathological examination of post-mortem brains: the problem of white matter high signal areas.** *Neuroradiology* 1994;36:393–98
4. Janota I, Mirsen TR, Hachinski VC, et al. **Neuropathologic correlates of leuko-araiosis.** *Arch Neurol* 1989;46:1124–28
5. Fernando MS, Simpson JE, Matthews F, et al, for the MRC Cognitive Function and Ageing Neuropathology Study Group. **White matter lesions in an unselected cohort of the elderly: molecular pathology suggests origin from chronic hypoperfusion injury.** *Stroke* 2006;37:1391–98
6. Murray AD, Staff RT, Shenkin SD, et al. **Brain white matter hyperintensities: relative importance of vascular risk factors in nondemented elderly people.** *Radiology* 2005;237:251–57. Epub 2005 Aug 26
7. Pantoni L, Garcia JH. **The significance of cerebral white matter abnormalities 100 years after Binswanger's report: a review.** *Stroke* 1995;26:1293–301
8. Fazekas F, Kleinert R, Offenbacher H, et al. **Pathologic correlates of incidental MRI white matter signal hyperintensities.** *Neurology* 1993;43:1683–89
9. Tomimoto H, Akiguchi I, Suenaga T, et al. **Alterations of the blood-brain barrier and glial cells in white-matter lesions in cerebrovascular and Alzheimer's disease patients.** *Stroke* 1996;27:2069–74
10. Hachinski V, Iadecola C, Petersen RC, et al. **National Institute of Neurological Disorders and Stroke-Canadian Stroke Network vascular cognitive impairment harmonization standards.** *Stroke* 2006;37:2220–41. Epub 2006 Aug 17
11. Miyazawa N, Satoh T, Hashizume K, et al. **Xenon contrast CT-CBF measurements in high-intensity foci on T2-weighted MR images in centrum semiovale of asymptomatic individuals.** *Stroke* 1997;28:984–87
12. Hatazawa J, Shimosegawa E, Satoh T, et al. **Subcortical hypoperfusion associated with asymptomatic white matter lesions on magnetic resonance imaging.** *Stroke* 1997;28:1944–47
13. O'Sullivan M, Lythgoe DJ, Pereira AC, et al. **Patterns of cerebral blood flow reduction in patients with ischemic leukoaraiosis.** *Neurology* 2002;59:321–26
14. Marstrand JR, Garde E, Rostrup E, et al. **Cerebral perfusion and cerebrovascular reactivity are reduced in white matter hyperintensities.** *Stroke* 2002;33:972–76
15. De Cristofaro MT, Mascalchi M, Pupi A, et al. **Subcortical arteriosclerotic encephalopathy: single photon emission computed tomography-magnetic resonance imaging correlation.** *Am J Physiol Imaging* 1990;5:68–74
16. Wardlaw JM, Sandercock PAG, Dennis MS, et al. **Is breakdown of the blood-brain barrier responsible for lacunar stroke, leukoaraiosis, and dementia?** *Stroke* 2003;34:806–12
17. Starr JM, Wardlaw J, Ferguson K, et al. **Increased blood-brain barrier permeability in type II diabetes demonstrated by gadolinium magnetic resonance imaging.** *J Neurol Neurosurg Psychiatry* 2003;74:70–76
18. Kemper TL, Blatt GJ, Killiany RJ, et al. **Neuropathology of progressive cognitive decline in chronically hypertensive rhesus monkeys.** *Acta Neuropathol* 2001;101:145–53
19. Aviv RI, Hopyan B, Mallia G, et al. *Computer Tomographic Perfusion Derived Permeability (permeability surface) Predicts Hemorrhagic Transformation: Proceedings of the International Stroke Conference, New Orleans, La, 20–22 February 2008.* New Orleans, La: American Heart Association; 2008
20. Wintermark M, Thiran J-P, Maeder P, et al. **Simultaneous measurement of regional cerebral blood flow by perfusion CT, and stable xenon CT: a validation study.** *AJNR Am J Neuroradiol* 2001;22:905–14
21. Kudo K, Terae S, Katoh C, et al. **Quantitative cerebral blood flow measurement with dynamic perfusion CT using the vascular-pixel elimination method: comparison with H2(15)O positron emission tomography.** *AJNR Am J Neuroradiol* 2003;24:419–26
22. Murphy BD, Fox AJ, Lee DH, et al. **White matter thresholds for ischemic penumbra and infarct core in patients with acute stroke: CT perfusion study.** *Radiology* 2008;247:818–25. Epub 2008 Apr 18
23. Murphy BD, Fox AJ, Lee DH, et al. **Identification of penumbra and infarct in acute ischemic stroke using computed tomography perfusion-derived blood flow and blood volume measurements.** *Stroke* 2006;37:1771–77
24. Wahlund LO, Barkhof F, Fazekas F, et al. **A new rating scale for age-related white matter changes applicable to MRI and CT.** *Stroke* 2001;32:1318–22
25. Cohnen M, Wittsack H-J, Assadi S, et al. **Radiation exposure of patients in comprehensive computed tomography of the head in acute stroke.** *AJNR Am J Neuroradiol* 2006;27:1741–45
26. Brenner DJ, Hall EJ. **Computed tomography: an increasing source of radiation exposure.** *N Engl J Med* 2007;357: 2277–84
27. O'Sullivan M, Rich PM, Barrick TR, et al. **Frequency of subclinical lacunar infarcts in ischemic leukoaraiosis and cerebral autosomal dominant arteriopathy with subcortical infarcts and leukoencephalopathy.** *AJNR Am J Neuroradiol* 2003;24:1348–54
28. Markus HS, Lythgoe DJ, Ostegaard L, et al. **Reduced cerebral blood flow in white matter in ischaemic leukoaraiosis demonstrated using quantitative exogenous contrast-based perfusion MRI.** *J Neurol Neurosurg Psychiatry* 2000;69:48–53
29. Powers WJ. **Cerebral hemodynamics in ischemic cerebrovascular disease.** *Ann Neurol* 1991;29:231–40
30. Bakker SL, de Leeuw FE, de Groot JC, et al. **Cerebral vasomotor reactivity and cerebral white matter lesions in the elderly.** *Neurology* 1999;52:578–83
31. Hassan A, Hunt BJ, O'Sullivan M, et al. **Markers of endothelial dysfunction in lacunar infarction and ischaemic leukoaraiosis.** *Brain* 2003;126:424–32
32. Roberts HC, Roberts TPL, Lee T-Y, et al. **Dynamic, contrast-enhanced CT of human brain tumors: quantitative assessment of blood volume, blood flow, and microvascular permeability—report of two cases.** *AJNR Am J Neuroradiol* 2002;23:828–32
33. Lin K, Kazmi KS, Law M, et al. **Measuring elevated microvascular permeability and predicting hemorrhagic transformation in acute ischemic stroke using first-pass dynamic perfusion CT imaging.** *AJNR Am J Neuroradiol* 2007; 28:1292–98
34. Zimny A, Sasiadek M, Leszek J, et al. **Does perfusion CT enable differentiating Alzheimer's disease from vascular dementia and mixed dementia? A preliminary report.** *J Neurol Sci* 2007;257:114–20